



# Discovery of the Romanesque church of the Abbey of our lady of Bec (Le Bec-Hellouin, Normandy, France) by means of geophysical methods

Cyrille Fauchard, Abdoulaziz Djibrila Saley, Christian Camerlynck, Yannick Fargier, Raphael Antoine, Paul-Franck Thérain

## ► To cite this version:

Cyrille Fauchard, Abdoulaziz Djibrila Saley, Christian Camerlynck, Yannick Fargier, Raphael Antoine, et al.. Discovery of the Romanesque church of the Abbey of our lady of Bec (Le Bec-Hellouin, Normandy, France) by means of geophysical methods. *Archaeological Prospection*, 2018, 25 (4), pp.315-328. 10.1002/arp.1711 . hal-01983346

HAL Id: hal-01983346

<https://normandie-univ.hal.science/hal-01983346>

Submitted on 9 Dec 2022

**HAL** is a multi-disciplinary open access archive for the deposit and dissemination of scientific research documents, whether they are published or not. The documents may come from teaching and research institutions in France or abroad, or from public or private research centers.

L'archive ouverte pluridisciplinaire **HAL**, est destinée au dépôt et à la diffusion de documents scientifiques de niveau recherche, publiés ou non, émanant des établissements d'enseignement et de recherche français ou étrangers, des laboratoires publics ou privés.

# Discovery of the Romanesque church of the Abbey of Our Lady of Bec (Le Bec-Hellouin, Normandy, France) by means of geophysical methods

Cyrille Fauchard<sup>a,b,\*</sup>, Abdoulaziz Djibrila Saley<sup>a,d</sup>, Christian Camerlynck<sup>e</sup>, Yannick Fargier<sup>c</sup>, Raphaël Antoine<sup>a,d</sup>, Paul-Franck Thérain<sup>f</sup>

<sup>a</sup>*Cerema, Equipe-Projet Evaluation Non Destructive des Structures et des Matériaux, END SUM, F-76121 Le Grand-Quevilly, France*

<sup>b</sup>*Université de Rouen Normandie, UMR 6634 GPM, F-76800 Saint-Etienne-du-Rouvray, France*

<sup>c</sup>*Ifsttar, GERS-RRO, F-69675 Bron, France*

<sup>d</sup>*Université de Rouen Normandie, UMR 6143 M2C, F-76821 Mont-Saint-Aignan, France*

<sup>e</sup>*Sorbonne Université, UPMC Univ Paris 06, CNRS, EPHE, UMR 7619 Metis, F-75005 Paris, France*

<sup>f</sup>*Direction Régionale des Affaires Culturelles de Normandie, F-76000 Rouen, France*

---

## Abstract

A geophysical survey was carried out in 2015 for the development of the patrimonial site of the Abbey of Our Lady of Bec (also called the Bec Abbey), located in Le Bec-Hellouin, Normandy, France. This survey aimed at optimizing the future accessibility programme by preserving the historical heritage of the Bec Abbey, taking into account potential underground remains. The ground penetrating radar (GPR), the electrical resistivity imaging (ERI) and the magnetic method (MM) were used to prospect the shallow surface. The GPR imaging shows longitudinal and curvated structures, drawing the classical and simplified plan of a Romanesque church basement of the 11th century. This is the most important discovery of this survey, since the existence of this church was historically known but has remained unlocated till this geophysical survey. The ERI measurements confirm and locally complete most of the GPR results. Despite the very magnetic-noisy environment, the MM investigation is the only method detecting a longitudinal structure that can be the foundation of an ancient wall between the Saint-Nicolas' tower and the church nave of the 13th century. Finally, authorities recently allowed in July 2017 the publication of excavations performed by archaeologists. Most of the geophysical anomalies have helped to target the archaeological investigation and the results provide a detailed interpretation in terms of depth and nature of remnants. Archaeological investigation then offers an important historical outcome of the various stages of construction and destruction of the Bec Abbey.

**Keywords:** Romanesque church, Ground Penetrating Radar, Electrical Resistivity Imagery, Magnetic Method

---

## 1. Introduction

In the past decades, geophysical methods have been increasingly used in archaeological studies for locating buried structures in the shallow surface (Rabbel et al. (2015); Zheng et al. (2013); Rodrigues et al. (2009); Drahor et al. (2011)) or for assessing walls condition of ancient buildings (Souffaché et al. (2015); Orlando et al. (2015); Brooke

---

\*Corresponding author

Email address: [cyrille.fauchard@cerema.fr](mailto:cyrille.fauchard@cerema.fr), Tel. +33235689295, Fax +33235688188 (Cyrille Fauchard)

5 (1994)). Various techniques can be carried out, depending on the area to survey, the depth of targets and the nature  
of the surrounding media. The best solution generally consists in (i) combining several geophysical methods with an  
accurate positionning system, (ii) observing on site details and (iii) gathering historical data from previous studies.  
For very large areas, an efficient approach consist in adding airbone and satellite remote sensing data such as aerial  
photography, spectral images, (Carr and Turner, 1996; Challis et al., 2009; Sarris et al., 2013), SAR (Sonnemann,  
10 2015) and LiDAR (Challis et al., 2011) data. McCoy and Ladefoged (2009) classify these techniques as a part of  
spatial technology applied to archaeology and underline the major development in prospecting subsoil by the use of  
geophysical methods. They also emphasize the various trends across the world concerning the use of geophysical  
methods in archaeological studies. Nevertheless, as some teams fully incorporate geophysical methods in research  
(Carr and Turner, 1996; Lowe and Fogel, 2010; Kvamme, 2003), others often move away such solutions because  
15 of a lack of communication between geophysicists and archeologists. Fortunaltely, reported works including the  
combination of geophysical methods for archaeological purposes are numerous. Some examples similar to our case  
study are described below.

Pérez-Gracia et al. (2009) carried out GPR, capacitively coupled resistivity method and seismic refraction to  
image the subsurface under and around the Cathedral of Mallorca (Spain). Whereas the GPR results lead to the three-  
20 dimensional imaging of underground features, resistivity and seismic refraction methods enhance the interpretation  
of the surrounding media. Papadopoulos et al. (2012) used various geophysical methods, including GPR, ERI and  
magnetic techniques for the mapping of the old ruins of a theatre and an ancient amphtheater in Crete. *A priori*  
information of an old map was superimposed on satellite views in order to detect old remnants. The combination of  
25 both the ERI and GPR surveys gave the most relevant results to image old relics in subsoils. More recently, Ranieri  
et al. (2016) combined magnetic, electromagnetic, electrical and GPR methods for the prospection of the Roman city  
of Pollentia.

This work presents a case study of a geophysical survey carried out in 2015 by means of GPR, ERI and MM  
techniques. It initially intends to offer useful information for archaeological prospection and to better target excava-  
tions. First, available data are collected from both the history of the Bec Abbey and the local geological map. Second,  
30 the basic principle of each geophysical method is reminded, as well as their data processing. An interpretation of  
underground anomalies is then proposed. Third, a discussion summarizes the main outcomes and drawbacks of the  
approach. A sketch of detected buried features with their interpretation is given, setting a precise map for archaeolog-  
ical prospecting. Finally, the recent excavations results obtained in July 2017 is partly presented, enlightening how  
35 geophysical methods lead to efficient excavations phase and how archaeological interpretation of discovered remnants  
give the right nature of geophyscial anomalies, as well as precious information on site history.

## 2. The history of the Bec Abbey

The Bec Abbey is located at the confluence of a stream and a river, the Bec and the Risle, respectively. The

reference work of the Bec Abbey history was written by Porée (1901). An historical work of paramount importance has been undertaken by Gazeau (2007) about the medieval and monastic intitutions in Normandy and the following 40 historical abstract of the Bec Abbey presents only the main building phases of this particular institution. The Bec Abbey building was undertaken in 1041 and Lanfranc de Pavie and Anselm largely contributed to its intellectual influence. The main building stages of the abbey can be summarized as follows:

- an important extension of the abbey and a church were respectively built in 1060 and 1063. This church of Romanesque architecture is called the 11th century church in this work;
- after the partial collapse of the church in 1197, a new building stage was developed;
- In 1274, the choir and the transept collapsed and an important construction plan undertook the creation of an imposing church and a monastery. This construction had continued till the 14th century. In the present work, this church is called the 13th century church;
- During the Hundred Years War, the site was fortified. After the war, the abbot Geoffroy d'Epargnes ordered the rebuilding of the abbey with many adjacent buildings (manors, barns, mills and an aqueduct) and the Saint-Nicolas' tower was built (see Figure 1, the *Monasticon Gallicanum*). Nowadays, this tower remains one of the 50 most outstanding architectural building of the abbey;
- During the 16th century, the nave collapsed, repairs and maintenance were no longer made, until the venue of a new monk community (congregation of Saint Maur) which started a new era of gigantic buildings in the 17th century: a cloister and the abbey housing were built in 1644 and in 1735, respectively. Other monastic edifices were built during the 18th century around the abbey, bringing back its erstwhile splendour, as shown in the 55 Figure 1;
- At the end of the 18th century, the abbey was abandoned and occupied by the army. In the 19th century, the church was used as a limestone quarry;
- In 1948, the site was bought by the French authorities and a new monk community has been settled in the abbey,

In the context of the patrimonial site development of the Bec Abbey, accessibility works are planed. Geophysical methods have been carried out on site, in order to (i) locate ancient remnants and (ii) optimize the excavation phase performed by archaeologists. This ultimate stage allows to trully assess the nature, depth and dimension of detected targets as well as to enrich and better understand the specific history of the Bec Abbey.

### 65 3. Geology

Taking into account the numerous stages of buildings of the Bec Abbey, it is obvious that the very near surface materials of the site must be composed of various backfilled materials, whose nature and physical properties are

unknown. As *a priori* information, the local geological map (Bignot et al. (1984)) of the studied site is detailed in the Figure 2 and consists of Albian to Quaternary formations respectively composed of:

- 70     • silty marls and ferruginous sands (Albian);  
      • Cenomanian to Coniacian chalks with flints;  
      • loess;  
      • alluvium.

The geophysical survey was mainly carried out on the modern alluvions formation composed of clayey silts and  
75     sands. It is obvious that the prospected soils present some heterogeneous and disturbed materials of anthropogenic activities. Dry sand and silt with low clay content can be considered as resistive materials, with a resistivity range from few dozens to few hundreds of  $\Omega \cdot m$ , taking into account the physical values of the most common earth materials encountered in geophysical survey reported in the work of Palacky (1988). Clay, clayey silt and peat are conductive materials with resistivity ranging from a few  $\Omega \cdot m$  to dozens of  $\Omega \cdot m$ . Finally, anthropogenic structures such as building  
80     basement are mainly made of limestone - extracted from the nearest quarries - that is considered as a relatively resistive material (typically about 100  $\Omega \cdot m$ ). In that context, GPR was chosen because it is suitable for the detection of such resistive structures, as long as they are close to the surface, and the surrounding materials resistive enough to create a detectable electromagnetic contrast. In order to efficiently complete the GPR results, ERI is used for the imaging both of resistive and conductive soils. Finally, the detection of other subsoils targets, such as materials containing  
85     Fe-oxydes related to antropogenic activities as well as disturbed soils, was performed by means of MM method.

#### 4. Geophysical measurements

##### 4.1. Surveyed area

An aerial view of the Bec Abbey is shown in the Figure 3. A red dotted line encircles the surveyed area, representing a prospected surface of about 6000  $m^2$ . As the presence of trees didn't allow a precise geolocalization of  
90     profiles during the survey, several Ground Control Points (GCP) were recorded with a Total Station System (Leica) for an accurate georeferencing of profiles. All the radar and MM profiles were oriented to a South-East to North-West direction and each profile direction was determined on site by a straight rope put on the surface, and displaced each time a new profile were surveyed. All obstacles (old building stones, trees ...) were bypassed, hence some surveyed radar zones contains blacked parts. The Figure 3 also reports the location of 8 ERI profiles. The position of the 13th  
95     century church basement and the outer wall of the abbey are drawn in doted and doted-dashed white lines, respectively, according to the visible remnants (cylindrical stones of ancient columns) present on site and to the representation of the abbey depicted in the Figure 1.

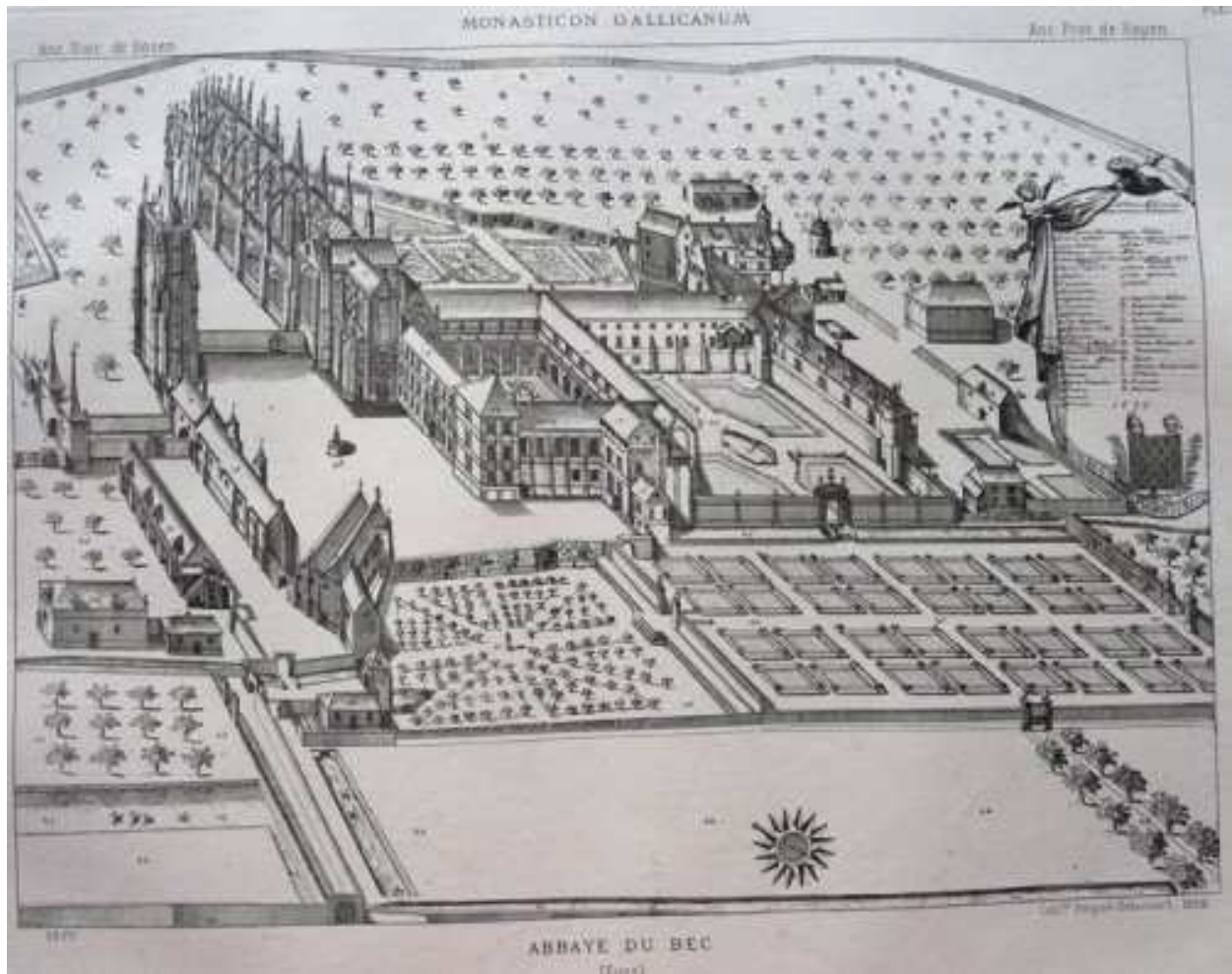
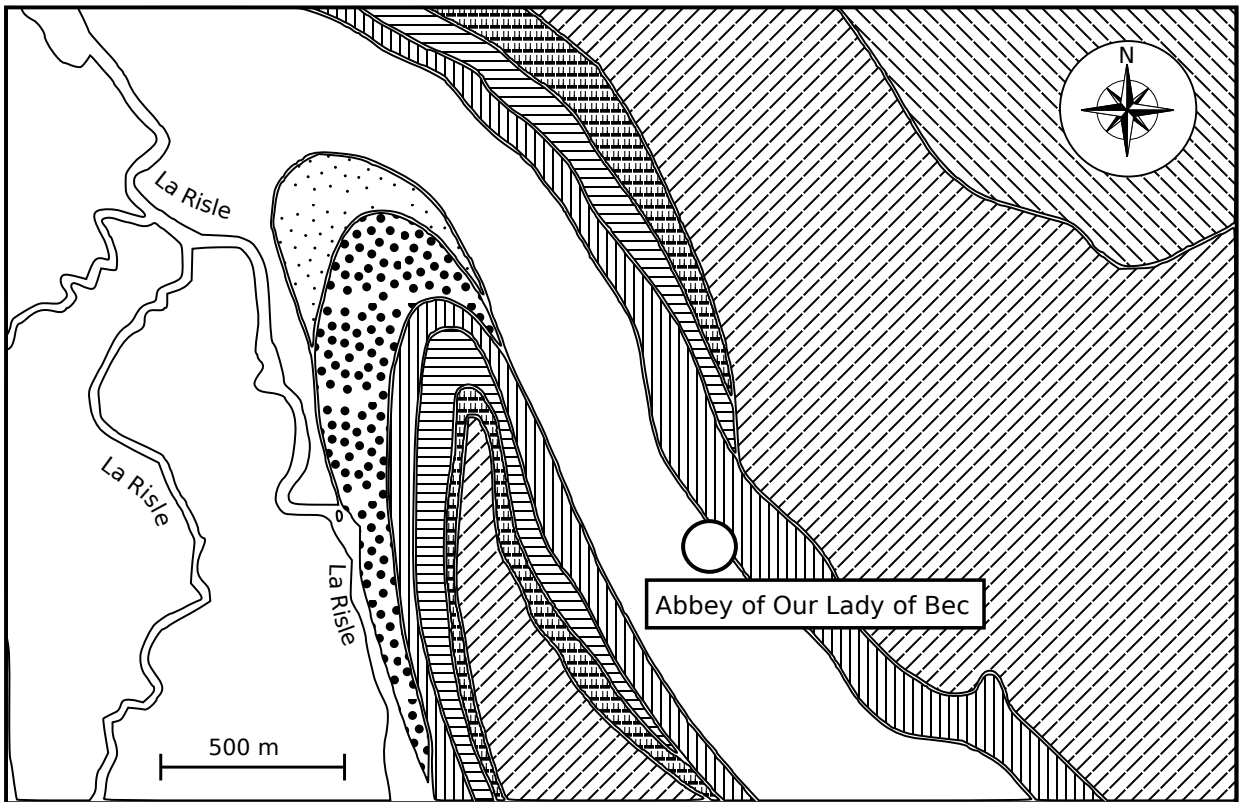


Figure 1: Monasticon Gallicanum de Dom Germain, Le Bec Héllouin, 1677 (Germain and Peigné-Delacourt, 1870).

#### 4.2. Ground Penetrating Radar

The basic principle of GPR ((Daniels, 2004)) is based on the propagation of electromagnetic waves emitted into a dielectric media. They reflect/scatter and refract at encountered dielectric contrasts. The reflected/scattered electric field is recorded at the surface by a receiver system. A time/frequency and amplitude analysis of waves allows the interpretation of dielectric contrasts as a spatial distribution of materials in the shallow surface. The result of a GPR measurement is an image - also called a B-scan - representing in x-axis, the distance followed at the surface, in y-axis, the two-way travel time of waves inside the soil, and in color scale the reflected/scattered amplitude. If several B-scan are recorded along a profile at a given distance, a 3D image can be reconstructed and represented in z-axis, as a x-y color map, the field strength proportional to encountered dielectric contrats related to materials distribution in the media.

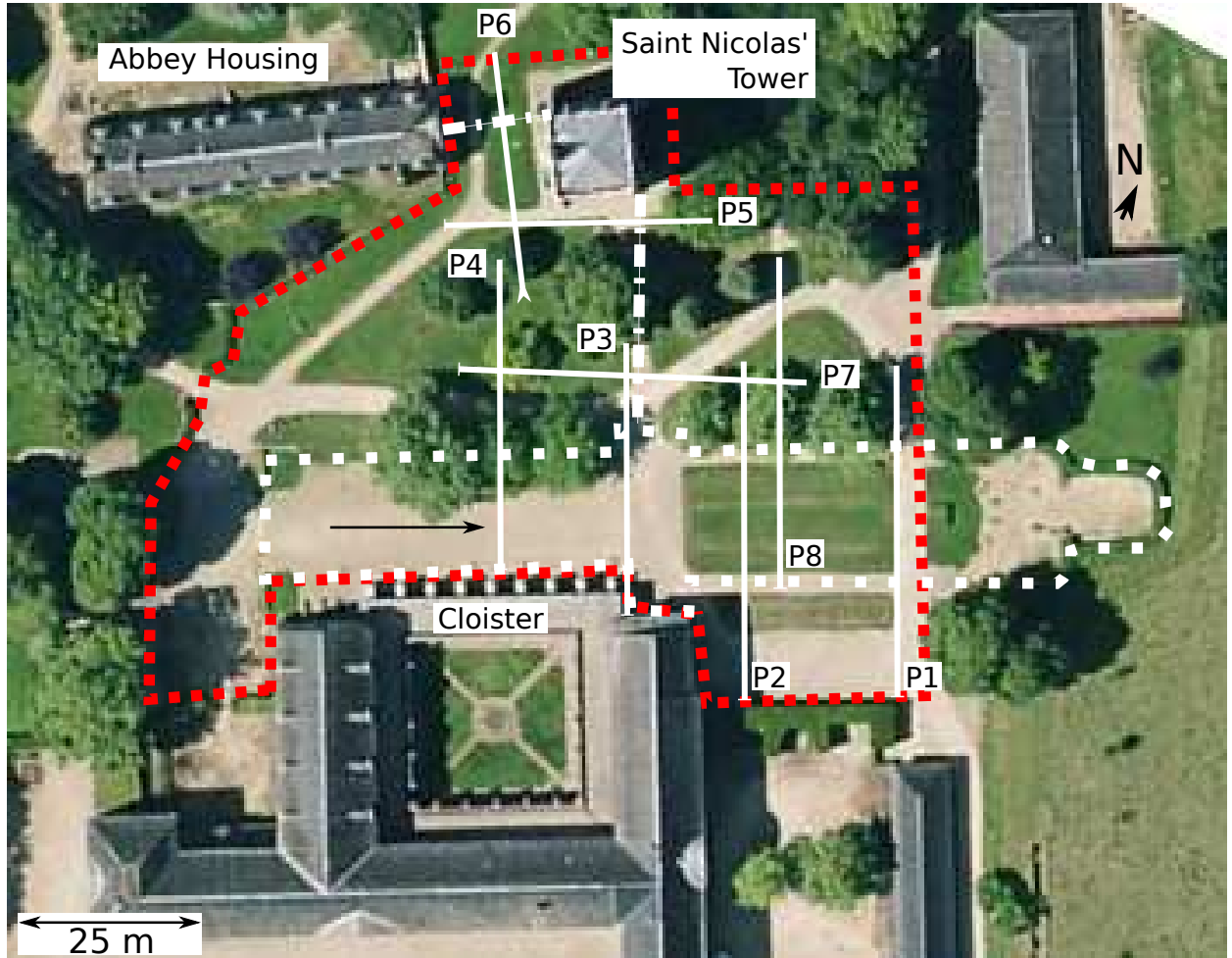
The GPR configurations in the field depends on the surface to prospect. In monostatic (Yaliner et al., 2009;



[Symbol: White box]	Modern alluvium : clayey silts, sand, clay, peat	[Symbol: Horizontal lines]	Turonian: grey chalk, marl with low content of flints
[Symbol: Dotted pattern]	Alluvial deposit	[Symbol: Vertical lines]	Coniacian-Santonian: white chalk with flints, foraminifera biozone
[Symbol: Dots pattern]	Slope loam	[Symbol: Diagonal lines]	Loess
[Symbol: Vertical lines]	Cenomanian: glauconitic chalk with grey and black flints	[Symbol: Cross-hatch]	Clay with flints

Figure 2: Geological map of the Abbey of Our Lady of Bec. The first centimeters of the shallow surface is mainly composed of anthropogenic materials and modern alluvium.

Castaldo et al., 2009) or bistatic mode (Booth et al., 2008), several parallel and transversal profiles defined on a grid at given space allow a 3D prospection and the result strongly depends on the space sampling. For large area (Trinks et al., 2010), multi-static configuration is preferred. In this experiment, the IDS Stream-X GPR solution is used with a 8-antenna system operating at 200 MHz (central frequency). Four emitter/receiver pairs, each antenna 12 cm separated, covering about 80 cm by swath, allow seven B-scan by pass. The Figure 4 shows the basic plan of the system and drawn B-scan and C-scan obtained over a particular area of interest described more in details here after. The distance sampling is 3.4 cm. This system was chosen (i) for its ability to efficiently survey a large area and (ii) for its frequency which allows an optimal depth of investigation of about 2 to 3 m depth in an unsaturated alluvial soil



- Hypothetic monastic walls location
- Hypothetic basement of the church of the 13th century
- Surveyed area with GPR and MM
- Resistivity profiles, 64 electrodes. P3-P6 : length = 44.1 m, spacing=0.7 m  
P1, P2, P7 and P8 : length=50.4 m, spacing=0.8 m

Figure 3: Aerial view of the Bec Abbey and studied area.

containing limestone foundations. The associated vertical resolution  $r$  can be approximated (Nyquist's law) by the following equation (Daniels, 2004):

$$r = \frac{\lambda}{4} \quad (1)$$

Where the wavelength  $\lambda = c f_c / \sqrt{\epsilon_r}$ ,  $c = 3.10^8 m/s$  is the speed of light in vacuum and  $\epsilon'_r$  is the dielectric constant, generally ranging from 5 to 15 for the considered materials. Hence, the vertical resolution approximately ranges from

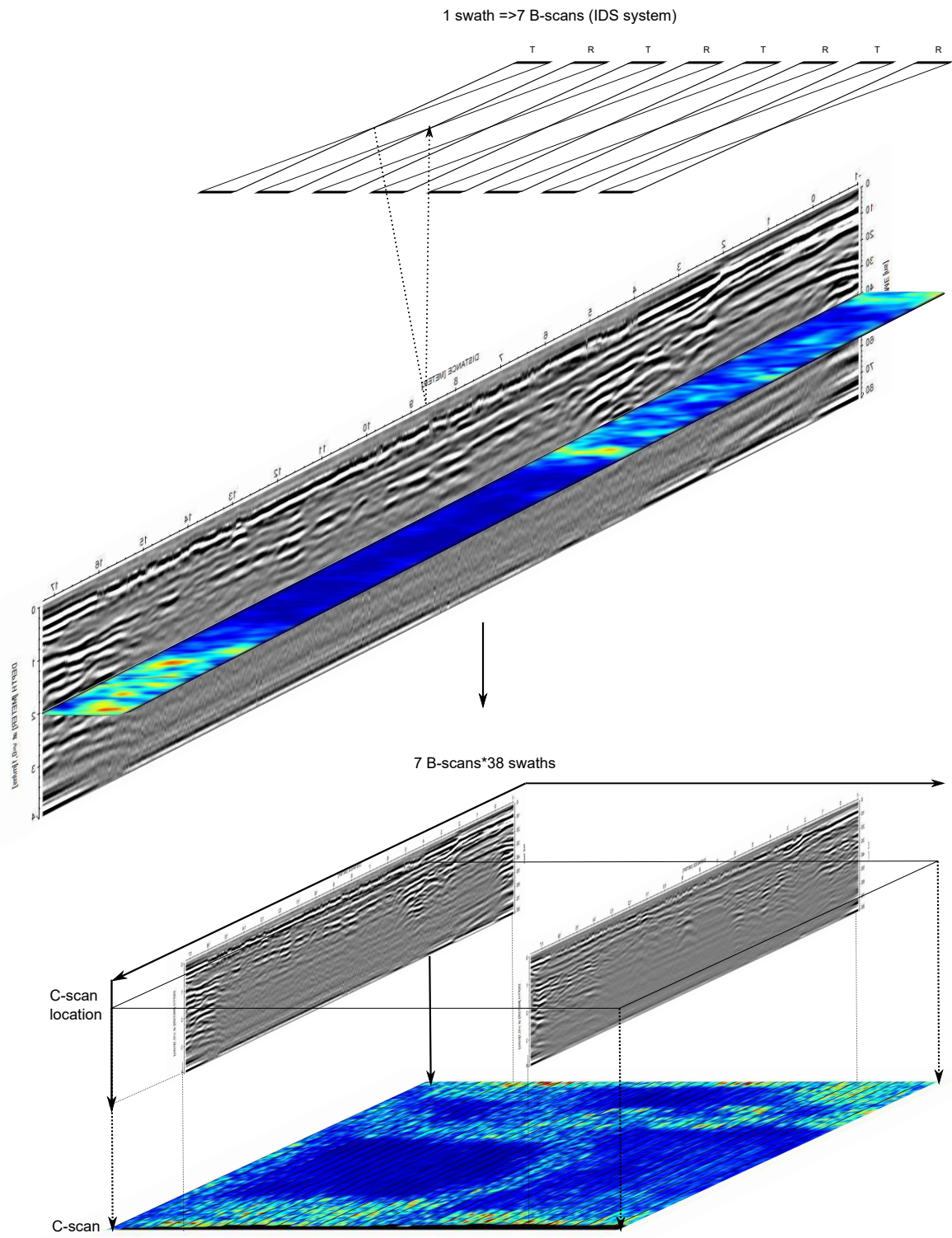


Figure 4: 3D-GPR principle, from B-scan, C-scan to GPR map (inspired from Ranieri et al. (2015)).

17 to 10 cm, respectively.

As the prospected surface is about 6000 m<sup>2</sup>, the large amount of data requires an adapted signal processing, provided by the GredHD software which allows a better interpretation of images. In that purpose, the following data processing is applied:

- a static correction for the initial time signal corresponding to the surface area;
- a gain filter for the visualization;
- a bandpass filter in order to remove unwanted frequencies;
- a background removal allowing noise reduction and antenna coupling effects;
- a migration to focus hyperbolae on punctual reflectors and to switch the data from time to depth;
- and a Hilbert transform ensuring an energy representation of signals.

Once the aforementioned data processing is applied, the 7-Bscan by pass are sampled in depth direction and the results obtained is a time slice (also called a C-scan) representing in x-y coordinates the area of the prospected surface, and in color scale the reflected amplitude of the radar signal. In this survey, the sampling is 512 points in depth. The approximated depth of investigation is about 3 m for a range of 70 ns and considering a real permittivity of 9 (meaning an approximate wave speed of 0.1 ns/m in the subsurface, without dielectric loss). The vertical spacing between each slice can be about 6 cm, allowing the user to select the slices at the desired depth of investigation.

The Figure 5 shows the C-scan at 0.3 m depth. It represents the beginning depth where electromagnetic signal is relevant and ground coupling effect is bypassed. Some features are visible. A long and thin NW-SE curve, starting from Saint Nicolas' tower to the right upper corner of the cloister is simply an electrical network for the lighting of the site. Other similar lines are pointed out in the Figure 5. Similarly a water network is detected at the western part of the survey. Other linear features are visible but their interpretation is uncertain. Edge effects can be seen in the eastern part of the survey, corresponding to the limits of surveyed sub-zones, alternatively covered by grass or sand and delineated by paths. At this depth, the detected anomalies are both connected to surface and shallow contrasts.

GPR slices at 1 m and 2m depth are shown in the Figure 6a) and 6b), respectively. Buried structures clearly appear at various locations. Remarkable reflectors in the lower central part to the eastern side draw straight features that can be the walls basement of ancient buildings, related to the 13th century church. The most outstanding part is located at the right upper corner of the cloister, and archaeologist experts can immediately recognize the basic plan of a Romanesque church basement, with the transept, the nave, a central chancel flanked by two small adjacent apses. This features remain visible to 2 m depth where the previous features are strongly marked by higher dielectric contrasts. The other features, probably related to basement of aisles church parallel to the nave and monastic buildings, can not be correctly interpreted without an archaeological analysis based on historical and architectural knowledges followed by excavation stage. Nonetheless, the main result of this GPR survey is the discovery of the Abbey of Our Lady of



Figure 5: GPR slice at 0.3 m depth.

Bec origins: the Romanesque 11th century church. The plan of this first Romanesque church is of major importance  
 155 for history and for cultural heritage in the context of further accessibility works which are planned in the near future.  
 Finally, according to the draw of the Figure 6c), the particular shape of the nave of 13th century church suggests it  
 was built right above the basement of the church of the 11th century.

#### 4.3. Magnetic method

The magnetic method is truly one the most common method used in archaeological prospecting (Chianese et al.  
 160 (2004); Barton and Fenwick (2005); Kvamme (2003); Dalan (2008)): it is a non-invasive, high resolution method  
 which allows rapid and extensive coverage of the study area. It is very sensitive (i) to old anthropogenic activities  
 related to materials transformation by means of fire (cooking, ferrous metallurgy, brickworks) (ii) and to subsurface  
 constraints between walls basement and other earthfill parts. We used a G-858 cesium magnetometer (Geometrics Ltd)

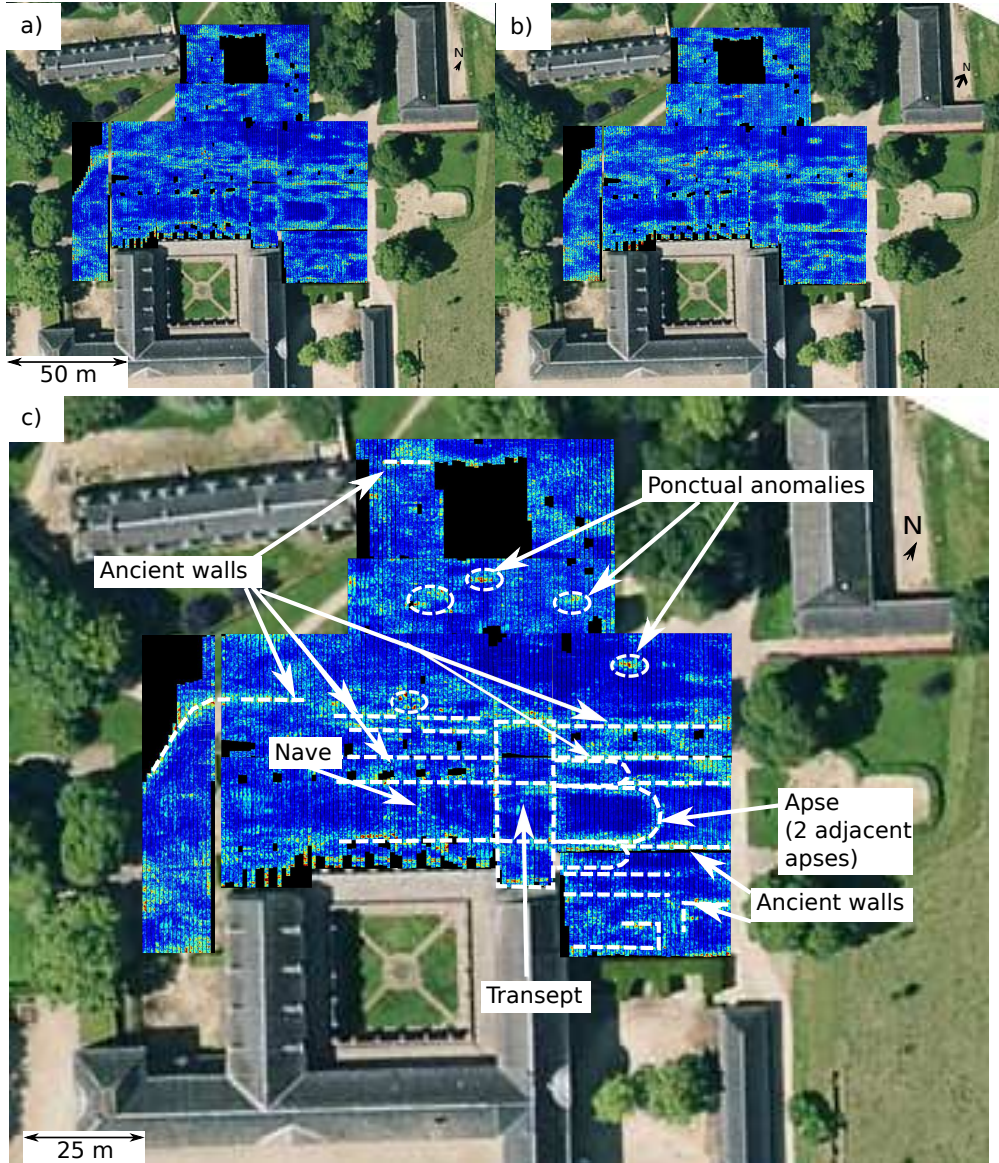


Figure 6: a) GPR slices at 1 m depth and b), at 2 m depth. c) Interpreted anomalies.

with 2 sensors in the vertical gradient configuration. This mode is commonly used in archaeological surveying; the  
 165 two sensors are fixed on an aluminum tube and separated vertically by a distance of 70 cm, the lower sensor being at 0.30 m elevation above the ground surface. The sensors are mounted on a an aluminum carriage allowing a constant sensor levelling and a regular displacement along profile. The difference between the values of the magnetic field intensity recorded by the two sensors divided by the distance between them approximates the vertical magnetic gradient measured at the midpoint between both sensors, also called the pseudo-vertical gradient. We prospected a surface area  
 170 of approximately 0.5 ha. Magnetic prospecting was carried out along a set of profiles separated by a distance of 1

m and made in opposite directions between adjacent profiles (zig-zag mode). On each profile measurements were made every 0.1 s, i.e. every 10 cm for an operator who moves with a speed of 3.6 km/h, the data acquisition system interpolating the data to correct variations in operator speed. The sensitivity of this type of magnetometers is 0.01 nT. For all geophysical surveys, before obtaining a simple result or interpretation, one have to clean the measured data  
175 to remove the effects induced by acquisition, external factors and defects of the devices; the removal of all effects not linked to buried archaeological structures is necessary and this pre-processing is particularly needed in magnetic geophysical prospecting. We applied the following corrections on the magnetic signal: spike-effect correction to remove spike anomalies often due to erroneous measurements on one of the sensors and herringbone effect correction to correct teeth-shaped anomalies (zig-zag effect) due to the profiling in opposite direction

In the Figure 7, the results of MM represent the magnetic field strength variations recorded over the surface, in nT. Magnetic variations may be caused by the presence of metallic structures, part of subsoils containing Fe-oxides or other magnetic rocks naturally present in the subsurface. According to the geological map, no natural magnetic materials can be found in the shallow surface. The magnetic anomalies detected on site are then mainly correlated with anthropogenic and modern activities.  
180

The magnetic map exhibits a long feature at the eastern part of the survey, related to the presence of a network under the path. This network was not detected by the GPR because this eastern part was not surveyed by GPR. A punctual anomaly is clearly revealed and is correlated with a punctual anomaly shown in the GPR (Figure 6c). Just at the top of the cloister, a rectangular feature can be correlated with the nave basement of the 13th century church. Another straight feature starting at the upper right corner of the previous rectangular anomaly, and ending at the bottom  
190 right corner of the Saint Nicolas' tower may be the signature of an ancient wall joining both buildings, as depicted in the reference document shown in the Figure 1). This feature is not detected in the radar survey. Nonetheless, even if this is less obvious than the discovery of the Romanesque church with the GPR survey, this magnetic signal is the only geophysical evidence that can be correlated with the wall drawn on the *Monasticon Gallicanum*. At last, the presence of strong magnetic anomalies around the Saint Nicolas's tower can be observed and only an archaeological  
195 survey based on excavation will allow a reliable interpretation. To sum up, the magnetic survey underlines three main anomalies: punctual features with one of them correlated with GPR, a rectangular zone that can be linked up to the nave of the 13th century church and a longitudinal feature that might be the basement of a disappeared wall. As far as concerned the depth of investigation of MM, the magnetic response of the shallow surface is linked to the presence of very near surface materials (less than 1m). Moreover, the magnetic contrast between materials is not correlated with dielectric contrast. Both reasons may partly explain why magnetic features strongly differ from near surface dielectric  
200 response.

#### 4.4. Electrical Resistivity Tomography

The ERI is another geophysical method commonly used for near surface studies. A set of conductive electrodes planted into the ground is implemented along a profile. The basic principle consists of a current injection through a pair

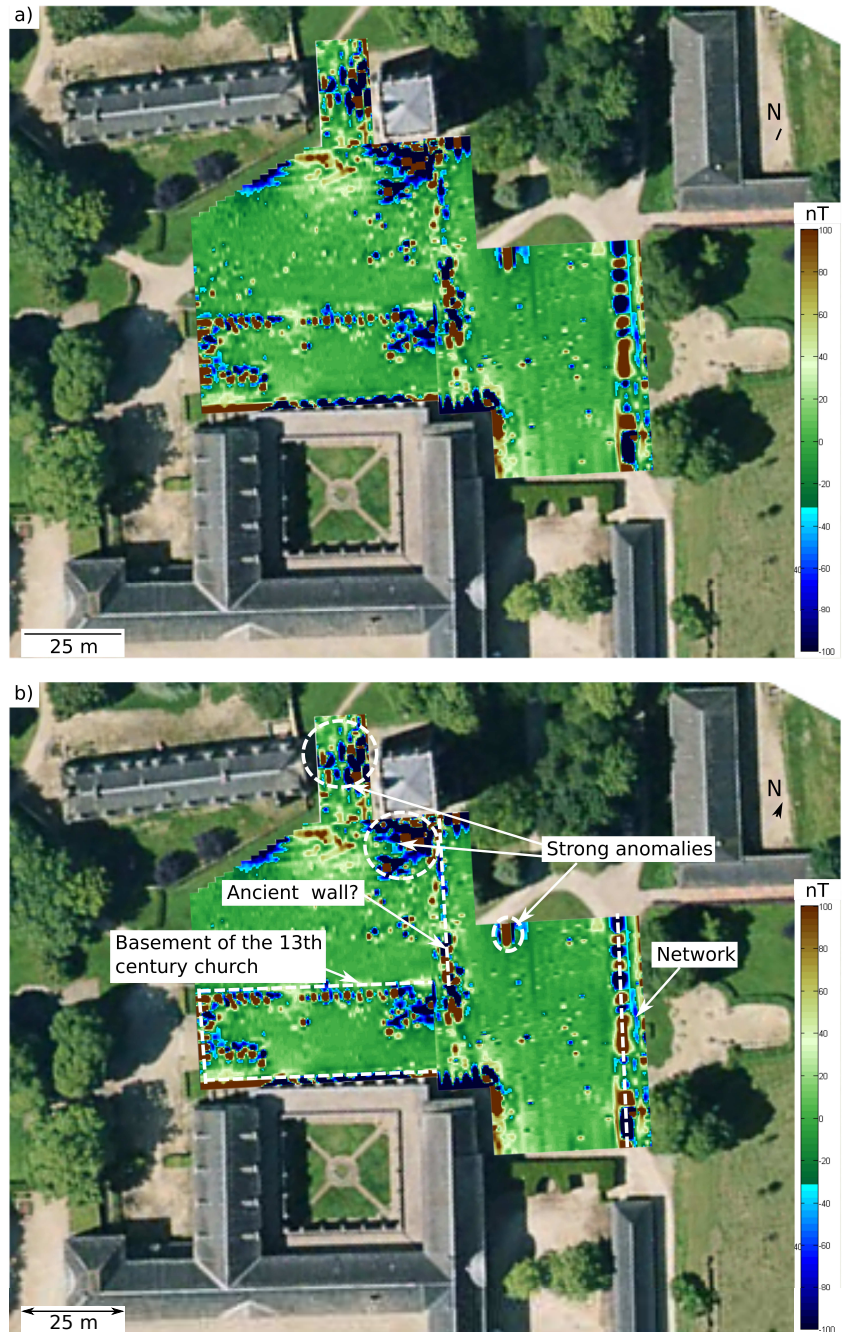


Figure 7: a) Raw magnetic survey and b), interpreted anomalies.

205 of electrodes and a voltage measurement with a different pair of electrodes. Various measurement configurations allow to emphasize vertical (Dipole-Dipole) or horizontal (Wenner) structures (Dahlin and Zhou, 2004). In this experiment,

the ERI survey was performed with a Terrameter LS system (ABEM) composed of 64 electrodes. 8 profiles (P1 to P8) were implemented according to the features detected with the radar survey. The P1, P2, P7, P8 and P3-P6 profiles have a 0.8 m (50.4 m length) and a 0.7 m (44.1 m length) electrodes spacing, respectively. The location of the profiles are shown in the Figure 3. Two configurations were used. The Wenner-alpha is good to image horizontal structures (vertical changes in resistivity), has a low signal-to-noise ratio but is relatively poor in detecting vertical structures, while the Dipole-Dipole is good to image the vertical structures (horizontal changes in resistivity) but relatively poor to image horizontal structures Loke (2001).

A classical data inversion processing (Loke and Barker, 1996; Dahlin, 1996) by means of the Res2DInv Software was applied to the recorded data and RMS criteria lower than 6% were reached as criteria to obtain reliable results (Loke, 2001). Most of the gathered data were of high quality and a quite perfect contact between electrodes was recorded, except for P4, P5 and P7 profiles with Dipole-Dipole configuration exhibiting noisy data at few electrodes. As well as vertical or horizontal features such as walls basement and pavements were expected, both Dipole-Dipole and Wenner data were analysed. A joint inversion of both results was also studied, according to authors such as Vega et al. (2003) who obtained an enhanced interpretation by jointly inverted Dipole-Dipole and Wenner arrays data. An example of the three kinds of results is shown in the Figure 8 for the IRE profile P2, located right above the supposed apse detected with GPR. As a global trend, both configurations offer valuable results: for the 44.1 m to 50.4 m long profiles, Dipole-Dipole and Wenner measurements lead to resistivity maps at 5 to 6 m depth, and 8 to 9 m depth, respectively. Joint resistivity maps generally show more details, combining the vertical resolution of Dipole Dipole and horizontal resolution of Wenner. Nevertheless, these techniques does not ensure the best imaging results as long as a detailed destructive inspection is not performed. Moreover, some alternative inversion techniques such as weighted inversion (Athanasios et al. (2007)) can lead to better results. In the context of this work, such approach was not necessary but could be undertaken in further studies.

For the sake of clarity, we choose to present the Wenner measurements which offer explicit results. As shown in the Figure 9, a perspective view of a satellite image combined with the radar slice at 1.5 m and the electrical results are represented. The ERI results are slightly over-elevated compared to the radar slice, in order to better compare the radar and electrical contrasts. The common 1.5 m depth of investigation between the radar and electrical methods is drawn as a dashed line. At this particular level, most of the GPR dielectric anomalies (red to sky-blue colors on GPR slice) correspond to resistive contrasts (orange-red to purple on Wenner images). Given the local geology and the historical data gathered, the resistive contrasts clearly reveal the presence of anthropogenic buildings: longitudinal features correspond to walls basement and are electrically resistive in the Wenner images, whereas the top soil is most of the time conductive (green and sky-blue colors). Moreover, very resistive anomalies located between 2 and 3 m depth, about 12 m large, on the P1, P8, P2, P3 and P4 profiles are aligned and exactly correspond to the nave basement of the 13th century church. A part of this basement can correspond to the chancel slab of the 11th century church, meaning that the 13th century gothic church was exactly built on the 11th century Romanesque church. In the figure 10, a focus is proposed to emphasize both the walls/nave basement of the two churches and also the basement of the

apse revealed by the GPR survey correlated with electrical images.

The P6 profile was measured between the Saint Nicolas' tower and the enclosure wall of the site and strong resistive contrasts are correlated with MM anomalies. Two profiles P5 and P7 were carried out transversally to the magnetic anomaly (wall basement) detected between the nave of the 13th century church and the Saint Nicolas' tower.  
 245 Very near surface electrical signal can be correlated with the magnetic anomaly. Nevertheless, the correlation between these two ERI profiles and MM/GPR results are not so obvious. First, electrode spacing (0.7-0.8 m) can be too large compared to the other methods sampling. Second, the electrical contrast is probably too low to be detected. Finally, the basement depth as shown by the corresponding excavation (see section 4.6)

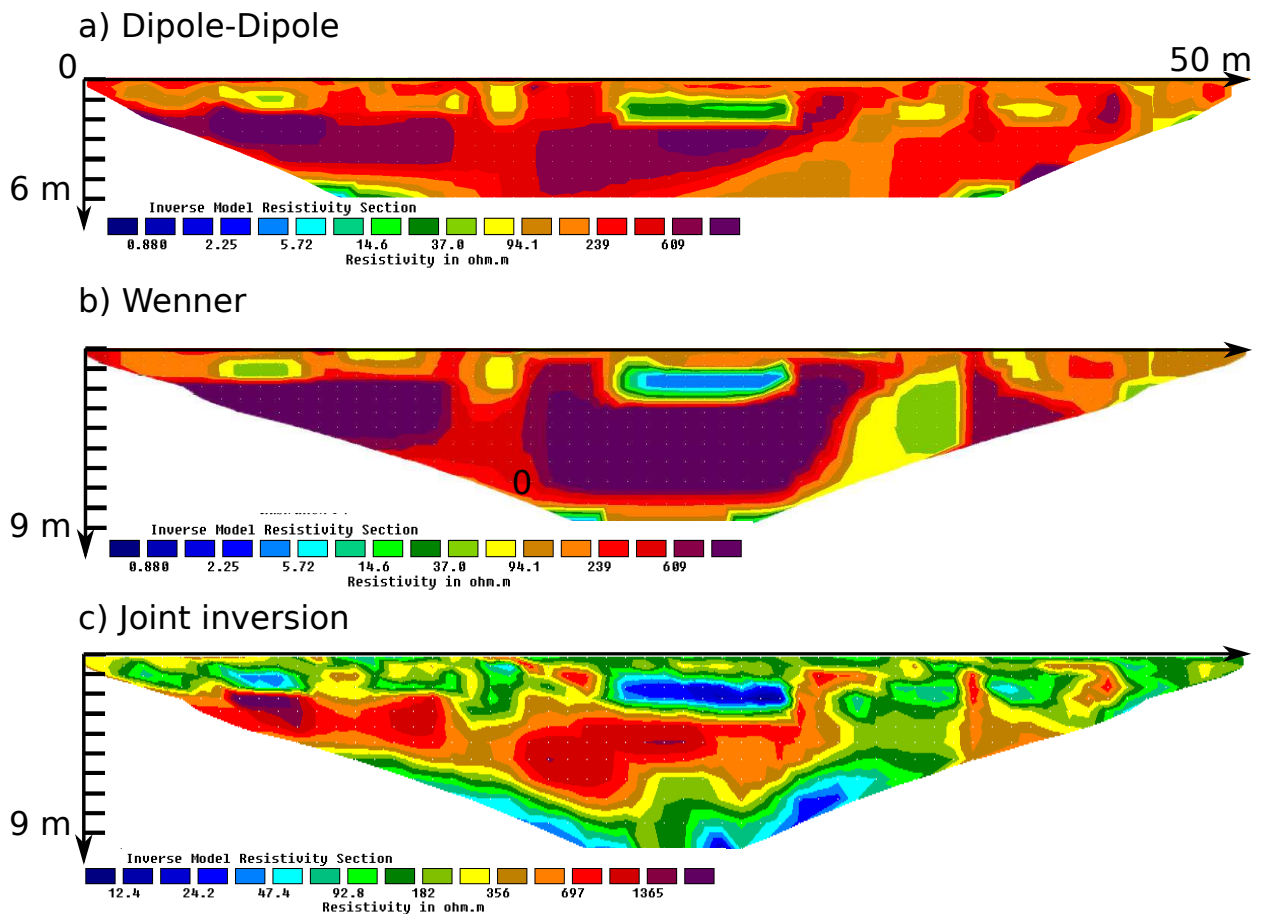


Figure 8: Comparison of IRE profile P2, a) Dipole-Dipole, b) Wenner and c) Joint inversion of Wenner and Dipole-Dipole data.

250 *4.5. Geophysical measurements conclusion*

Tacking account for the main results of GPR, MM, and ERI methods, a sketch of the main geophysical anomalies are depicted in the figure 11. It is important to note that this interpretation is provided as a priori information to archaeologists. A deeper analysis is conducted in the next excavation section.

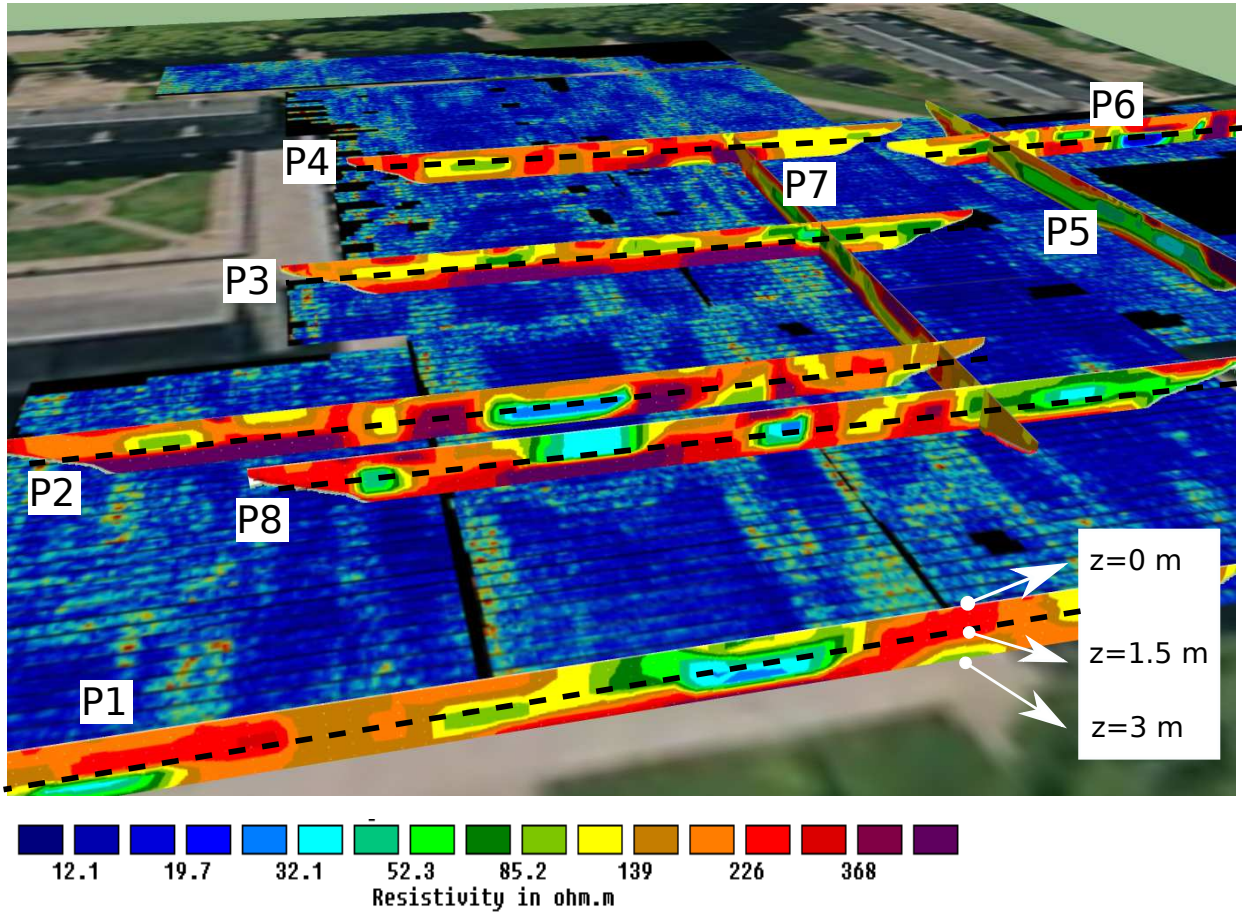


Figure 9: Superimposition of 8 Wenner images and the radar slice at 1.5 m depth. The black-dashed lines reported on each resistivity image is the 1.5 m depth of the radar slice.

#### 4.6. Excavation trenches

During spring 2015, excavation trenches have been carried out on site and the results have been recently presented in June 2017 by Deshayes (2017). 28 excavation trenches were performed close to or just above the anomalies detected by means of geophysical methods. This work is also based on a deep historical research recounting the various phases of construction and destruction that have left their mark on the Bec abbey history. As the amount of results is accurately detailed in the archaeological report, we choose to present some of the most pertinent results where geophysical measurements indicated potential targets as well as where none of these methods were efficient.

Considering the GPR results and the obvious arch shape imaged by the method, the excavation trenches shown in the two photos noted S1 and S2 ( $24 \text{ m}^2$ ) in the Figure 12 were undertaken at the top part of the supposed Romanesque church abside. In the photo S1, two wall basements composed of silex and limestone elements, banded with a pink-orange mortar, are visible. They are 0.5 m depth, 1.7 and 2 m width, separated by a brown silt part of 10.3 m long. They represent also the wall foundation of the gothic church built in the 13th century. S2 exhibits a wall basement,

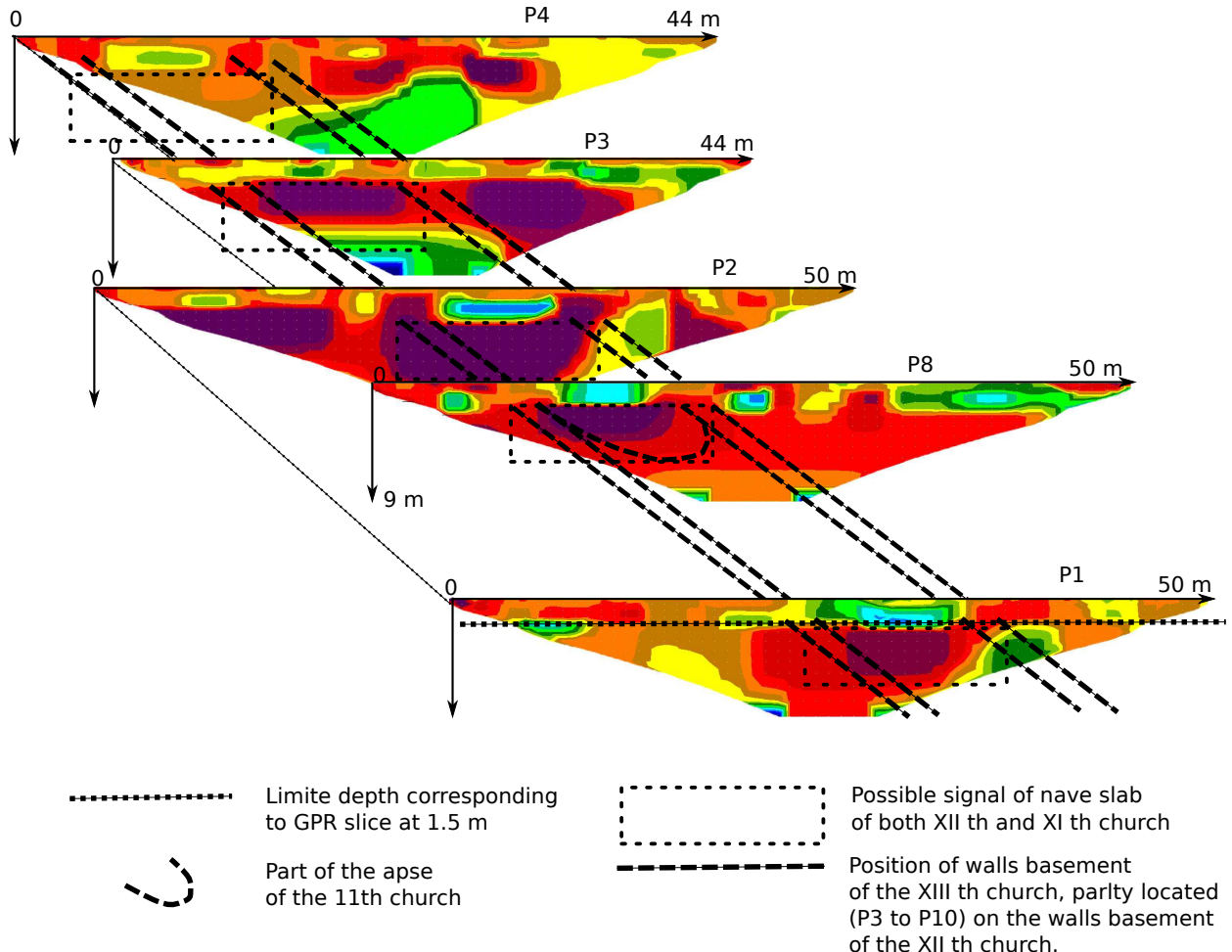


Figure 10: 5 Wenner profiles (P1-4 and P8) and sketch of the apse of the original Romanesque church surrounding by two longitudinal features that correspond to the walls basement of the 11th till P8, and to the walls basement of 13th church beyond.

2.7 m width at 0.5 m depth, composed of silex binded by a yellow mortar. This discovery, exactly located on the corresponding GPR anomaly is probably the oldest remnant revealed during this campaign. It corresponds to the top apse of the 11th century Romanesque church. Moreover, the excavation trench revealed a grave in the church axis-oriented, buried after the Romanesque church destruction, in the middle of the gothic choir, indicating the burying of  
270 an important person of the middle 12th century.

The photos S3 shows an excavation trench ( $11 \text{ m}^2$ ) performed transversally over the east bay of the chapter room. Its depth reaches 1.46 m. From the top-left to the bottom-right, two basements walls composed of limestones blocks binded with mortar and separated by 0.9 m width of brown silt delimited the east chapter room and its gutter. At the bottom right of S3, (i) some limestones blocks of the chapter room collapsed arch and (ii) a grave with foot bones  
275 were found. Various blocks and remains were also discovered allowing a dating of these remnants during the 12th

### 11th century church

- a) nave basement
- b) transept
- c) apse (and adjacent apses)

### 13th century church

- d) nave basement

### Other features

- e) closing wall basement
- f) local GPR anomalies
- g) local MM anomalies
- h) basement of the closing wall between Saint Nicolas' tower and the nave of the 13th century church
- i) other foundations

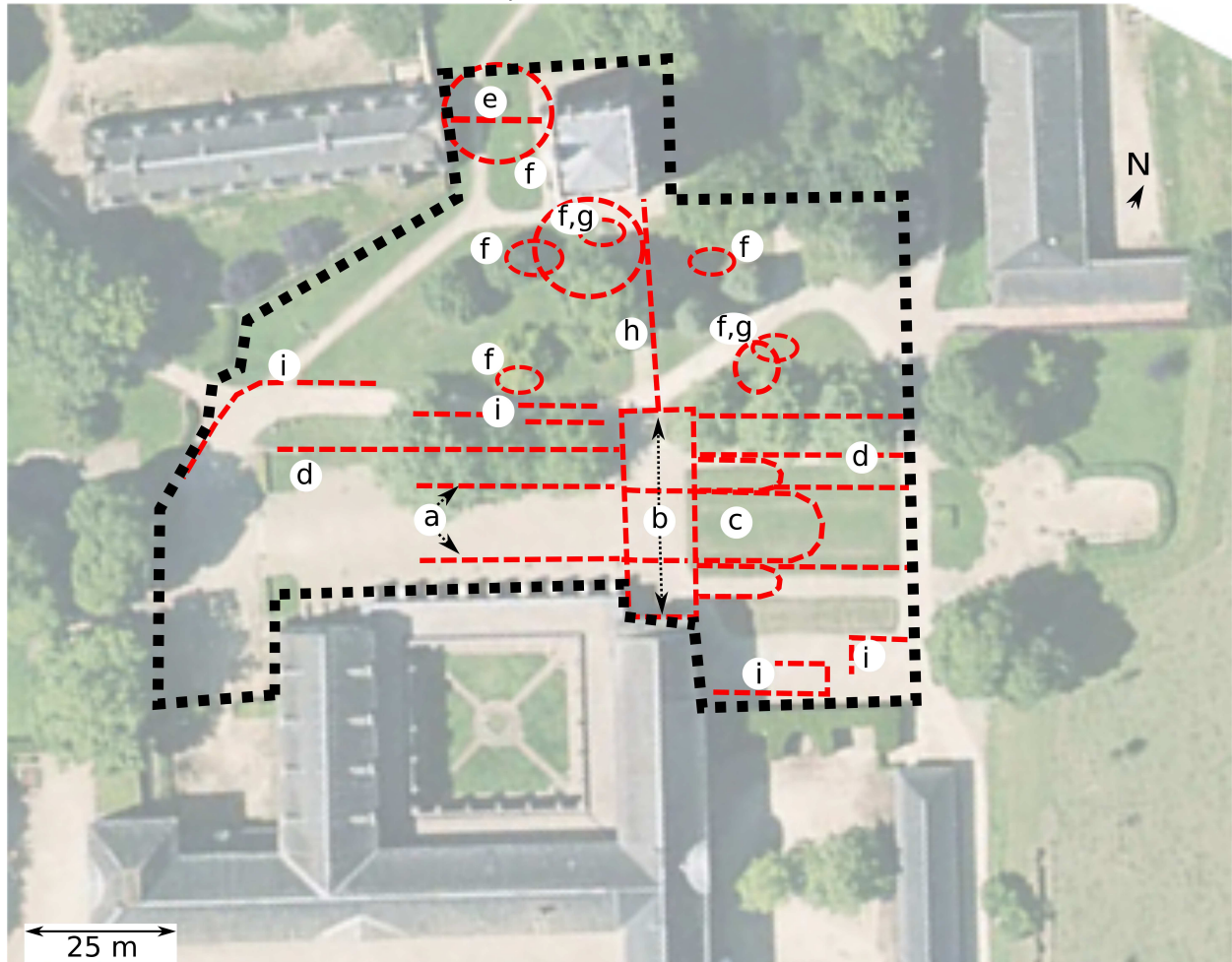


Figure 11: Sketch of the main geophysical anomalies (in red-dashed line). In black-dotted line, the prospected area as depicted in the Figure 3.

century.

The excavation trench S8 ( $7 \text{ m}^2$ ) mainly exhibits two structures. First, at the top of the photo, the pavement ground of the nave is composed of a grey silt and various limestone gravels. At the bottom of the picture, the basement wall of 2.96 m width composed of limestone blocks, banded with pink mortar revealing the front wall of the gothic abbey. Considering the various shapes and origins of the blocks composing this basement, these various elements

correspond to a rebuilt phase dating back the middle of the 17th century.

The excavation trenche S7 was performed at the supposed location of the north-west pillar between the nave and the transept. Six levels of masonry have been analysed, describing the abbey building and destruction history from the 11th to the near XXth century.

285 The excavation trenche S6 ( $9 \text{ m}^2$ ), 1.2 m max depth, shows a 0.45 m width water network buried in a limestone layer and paved with limestones blocks. It was probably linked to the cloister dating from the 17th century.

GPR anomalies exist at S3, S6, S7 and S8 locations, but only the archaeological excavation trenches reveal the true nature of materials.

Finally, two excavation trenches buried right above supposed walls basement are presented. At these locations the 290 MM method detected strong signals. The excavation trenche S5 ( $5 \text{ m}^2$ , 0.9 m max depth) has been buried in order to detect the wall between the Saint Nicolas' tower and the abbey outer wall. A 1.6 m width wall of limestone blocks binded with pink-orange mortar is revealed. It is probably dating from the Hundred Years War Deshayes (2017). The excavation trenche S4 ( $3 \text{ m}^2$ , 0.3 m max depth) was especially buried in order to reveal the outer wall basement linking the Saint Nicolas' tower and the abbey transept. The excavation trenche shows here a 1.2 m width wall of limestones 295 and silex blocks binded with yellow mortar. It is dated from the middle of 15th century. It is noticeable that magnetic method revealed a positive and elongated anomaly corresponding to this wall basement. We suppose both that this basement is too close to the surface (ground coupling effect) and its dielectric contrast too low to be detected by GPR.

All the 28 excavation trenches performed on site also show how rich is the history of the Bec Abbey and a complete analysis is described in the work of Deshayes (2017).

300 **4.7. Discussion**

The GPR method is clearly the most efficient tool used during this survey. Its ability to quickly investigate an 6000  $\text{m}^2$  area with an optimal depth of investigation up to 2.5 m represents a powerful approach to this archaeological case study. Indeed the local geology is favourable: the top surface is mainly composed of resistive and backfilled materials. Moreover, the very shallow depth of the remnants confirmed by archaeological excavation trenches facilitates the 305 geophysical detection. This case study illustrates the powerful capabilities of GPR for detecting and precisely mapping buried stones and remnants (Camerlynck et al., 1994) compared to more integrative ERI and MM methods. However, the method doesn't provide any result in conductive soils. In addition, the cost time of GPR data processing can be very important for such a surface and obtaining a relevant C-scan on the whole site requires high hardware ressources. As a main result and confirmed by S1/S2 excavation trenches, this GPR campaign has revealed the position of an 310 ancient Romanesque church that the trace was lost with time, as well as many other features, often linear, correlated with the basement of disappeared walls of various buildings of the abbey. The identification of the apse (and probably its two little adjacent apses) is definitely the most impressive result of this campaign. The excavation trenches S1/S2 gives an accurate depth and precise the nature of this basement. In the counter part, the wall between the Saint Nicolas'

315 tower and the transept were not detected with GPR and the S4 excavation trenche results suggest that this basement is too close to the surface to be detected by GPR, as it is located in the ground coupling depth.

The MM was carried out for its workability and its ability to map in a short time (few hours) the whole surface. The main drawback of the method is its sensitivity to near surface networks and to any metallic features on the surface. In the present case study, a straigth feature exactly corresponds to the basement of an ancient wall (S4 excavation trenche) linking the nave of the 13th church and the Saint Nicolas' tower, as depicted by historical data.

320 The ERI completes the previous measurements as it provides some information deeper than GPR and magnetic methods. It is also more sensitive to the changing of materials inside the soil, as the measured parameter, the so-called apparent resistivity, varies on a large scale of values, allowing the imaging of conductive (clayey earth) to resistive (limestone basement) materials. As the ERI campaign was directly planned before the GPR survey interpretation, the ERI profiles location can seem to be not optimal and other parts of the site would surely deserve to be imaged  
325 by this technique. Fortunately, and according to the historical data and on site observation, most of the profiles are relevant, showing electrical contrasts perfectly correlated with the GPR results. Moreover, the ERI shows a subsurface containing many rectangular and elongated features. The correlation between profiles suggests the presence of a slab (resistive anomaly) under the nave of both churches. Excavation depth of investigation did not allow to confirm this hypothesis.

330 **5. Conclusion**

A geophysical campaign has been undertaken to prospect the surroundings of the Bec Abbey by means of geophysical methods. The aim was to optimize the accessibility programme by locating possible remnants of major interest in the underground. For that purpose, historical and geological data has been gathered to choose the most relevant geophysical methods. The GPR, ERI and MM techniques have been carried out, covering an area of 6000 m<sup>2</sup>. The  
335 main outcome of the GPR survey is the discovery of the original Romanesque 11th century church, by imaging the apse and its adjacent buildings. Many other straight features are detected, corresponding most of the time to ancient walls basement of both the 11th and the 13th centuries churches. The magnetic survey underlines a signal that fits exactly the position and an ancient wall between the Saint Nicolas' tower to the nave of the 13th church, as depicted by a historical data of the abbey. Finally, the ERI prospection confirms the location of various buidling basements  
340 detected by the GPR survey. Moreover, it locally provides a detailed and deeper imaging of the subsoil as well as a more complete description of the material distribution: walls basement is drawn and the nave slab of the both churhes are described by a very resistive anomaly. The excavation stage was mainly conducted according to geophysical results and historical data. In particular archaeological prospection confirms the presence of the Romanesque church basement. Moreover, it enriches the building history of the Bec Abbey by providing a detailed analysis of materials  
345 detected by geophysical methods.

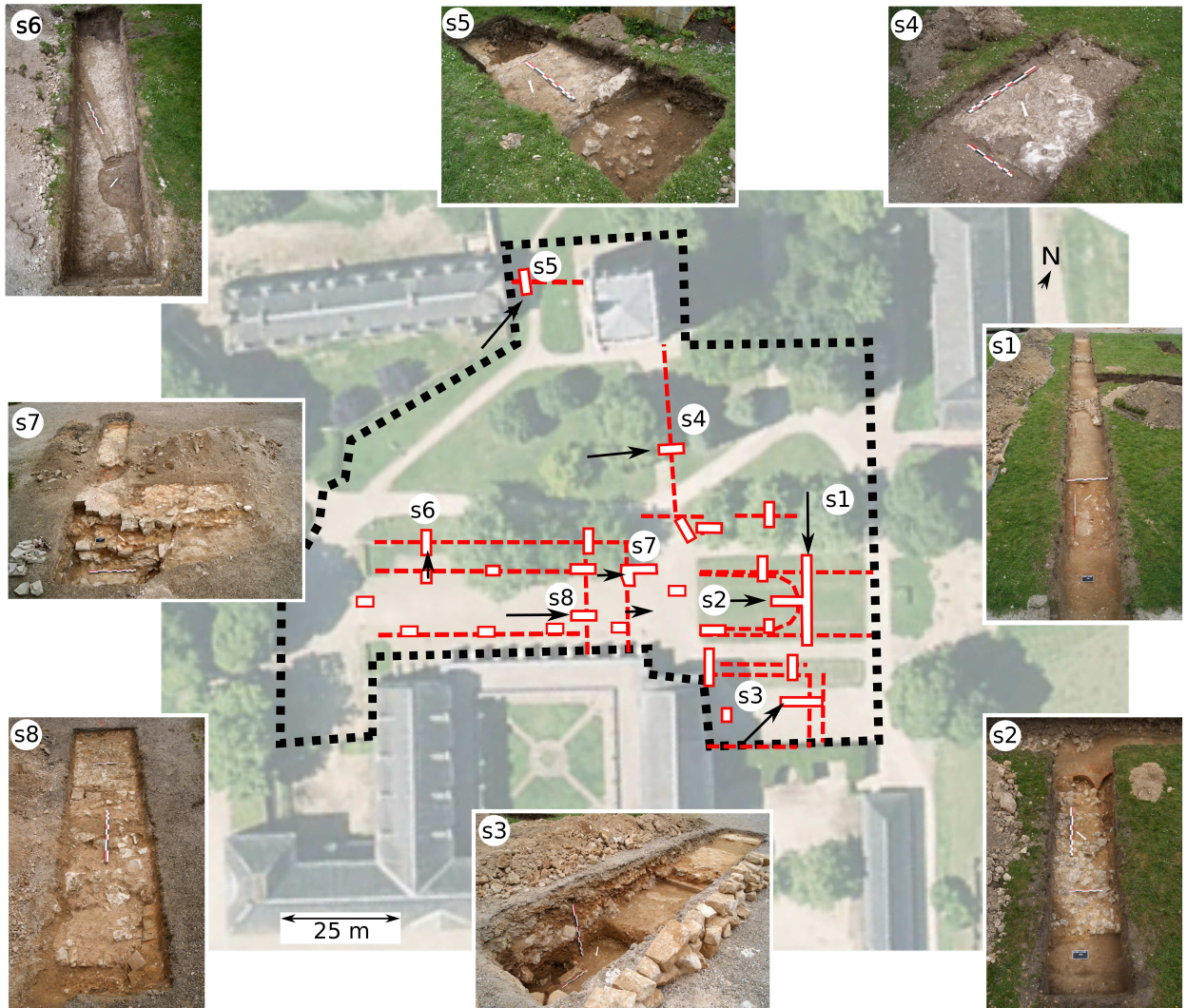


Figure 12: 28 excavation trenches (white polygons in red contour) on the prospected area (in black-dotted line). The black arrows indicate the excavation trenches point of vue. The red-dotted lines are various wall basements confirmed by the archaeological prospection. All excavation trenches and photos were performed by Deshayes (2017)

## 6. Authors contribution

Cyrille Fauchard as corresponding author managed the geophysical survey, the final data processing, the proposed interpretation, wrote the article and realized all the figures, except figure 1. Abdoulaziz Djibrilla Saley, as Ph.D Student in Rouen Normandy University, realized the geophysical measurements, the data processing and proposed a first interpretation through french technical report. Yannick Fargier supervised the ERI section and reviewed the whole article. Christian Camerlynck realized the magnetic measurements, treated the data and supervised the magnetic section of the article. Raphaël Antoine realized the ERI measurements and reviewed the whole article. Paul Franck

Thérain managed the whole project in the context of the rehabilitation of the Bec Abbey surroundings and reviewed the historical part of the article. We are very grateful to the reviewers for the proposed improvements.

355 **7. Acknowledgments**

The authors would like to thank the Regional Direction of Cultural Heritage of Normandy who permitted this geo-physical study and Gilles Deshayes who realized the excavation trenches and allowed an enhanced interpretation. We are particularly thankful to the monks of the Bec Abbey who welcomed us on site, provided us precious information on the site history and who were the first to suggest the discovery of the Romanesque church when we shown us our 360 first results on site. The authors also would like to thank Cyril Ledun, Vincent Guilbert, Quentin Wojchewski, Cécile Mézon, Bruno Beaucamp and Rodolphe Duval for their participation to the geophysical survey.

## References

- Rabbel, W., Erkul, E., Stmpel, H., Wunderlich, T., PaÅteka, R., Papco, J., et al. Discovery of a byzantine church in iznik/nicaea, turkey: an educational case history of geophysical prospecting with combined methods in urban areas. *Archaeological Prospection* 2015;22(1):1–20. URL: <http://dx.doi.org/10.1002/arp.1491>. doi:10.1002/arp.1491; aRP-14-0004.R1.
- Zheng, W., Li, X., Lam, N., Wang, X., Liu, S., Yu, X., et al. Applications of integrated geophysical method in archaeological surveys of the ancient shu ruins. *Journal of Archaeological Science* 2013;40(1):166–175. URL: <http://www.sciencedirect.com/science/article/pii/S0305440312003731>.
- Rodrigues, S.I., Porsani, J.L., Santos, V.R., DeBlasis, P.A., Giannini, P.C.. Gpr and inductive electromagnetic surveys applied in three coastal 370 sambaqui (shell mounds) archaeological sites in santa catarina state, south brazil. *Journal of Archaeological Science* 2009;36(10):2081–2088. URL: <http://www.sciencedirect.com/science/article/pii/S0305440309001733>.
- Drahor, M.G., Berge, M.A., -ztrk, C.. Integrated geophysical surveys for the subsurface mapping of buried structures under and surrounding of the agios voukolos church in zmir, turkey. *Journal of Archaeological Science* 2011;38(9):2231–2242. URL: <http://www.sciencedirect.com/science/article/pii/S0305440311001105>.
- Souffaché, B., Kessouri, P., Blanc, P., Thiesson, J., Tabbagh, A.. First investigations of in situ electrical properties of limestone blocks of ancient 375 monuments. *Archaeometry* 2015;n/a-n/aURL: <http://dx.doi.org/10.1111/arcm.12204>. doi:10.1111/arcm.12204.
- Orlando, L., Cardarelli, E., Cercato, M., De Donno, G.. Characterization of a pre-trajan wall by integrated geophysical methods. *Archaeological Prospection* 2015;22(3):221–232. URL: <http://dx.doi.org/10.1002/arp.1509>. doi:10.1002/arp.1509; aRP-14-0042.R1.
- Brooke, C.J.. Ground-based remote sensing of buildings and archaeological sites: Ten years research to operation. *Archaeological Prospection* 380 1994;1(2):105–119. URL: [http://dx.doi.org/10.1002/1099-0763\(199412\)1:2<105::AID-ARP6140010204>3.0.CO;2-F](http://dx.doi.org/10.1002/1099-0763(199412)1:2<105::AID-ARP6140010204>3.0.CO;2-F). doi:10.1002/1099-0763(199412)1:2<105::AID-ARP6140010204>3.0.CO;2-F.
- Carr, T.L., Turner, M.D.. Investigating regional lithic procurement using multi-spectral imagery and geophysical exploration. *Archaeological Prospection* 1996;3(3):109–127. URL: [http://dx.doi.org/10.1002/\(SICI\)1099-0763\(199609\)3:3<109::AID-ARP52>3.0.CO;2-P](http://dx.doi.org/10.1002/(SICI)1099-0763(199609)3:3<109::AID-ARP52>3.0.CO;2-P). doi:10.1002/(SICI)1099-0763(199609)3:3<109::AID-ARP52>3.0.CO;2-P.
- Challis, K., Kincey, M., Howard, A.J.. Airborne remote sensing of valley floor geoarchaeology using daedalus atm and casi. *Archaeological Prospection* 385 2009;16(1):17–33. URL: <http://dx.doi.org/10.1002/arp.340>. doi:10.1002/arp.340.
- Sarris, A., Papadopoulos, N., Agapiou, A., Salvi, M.C., Hadjimitsis, D.G., Parkinson, W.A., et al. Integration of geophysical surveys, ground 390 hyperspectral measurements, aerial and satellite imagery for archaeological prospection of prehistoric sites: the case study of Vésztö-Mágör Tell, Hungary. *Journal of Archaeological Science* 2013;40(3):1454–1470. URL: <http://www.sciencedirect.com/science/article/pii/S0305440312004827>.

- Sonnemann, T.F.. Spatial configurations of water management at an early Angkorian capital - combining GPR and TerraSAR-X data to complement an archaeological map. *Archaeological Prospection* 2015;22(2):105–115. URL: <http://dx.doi.org/10.1002/arp.1502>. doi:10.1002/arp.1502.
- Challis, K., Carey, C., Kinsey, M., Howard, A.J.. Airborne lidar intensity and geoarchaeological prospection in river valley floors. *Archaeological Prospection* 2011;18(1):1–13. URL: <http://dx.doi.org/10.1002/arp.398>. doi:10.1002/arp.398.
- McCoy, M.D., Ladefoged, T.N.. New developments in the use of spatial technology in archaeology. *Journal of Archaeological Research* 2009;17(3):263–295. URL: <http://dx.doi.org/10.1007/s10814-009-9030-1>. doi:10.1007/s10814-009-9030-1.
- Lowe, K.M., Fogel, A.S.. Understanding northeastern plains village sites through archaeological geophysics. *Archaeological Prospection* 2010;17(4):247–257. URL: <http://dx.doi.org/10.1002/arp.394>. doi:10.1002/arp.394.
- Kvamme, K.L.. Multidimensional prospecting in north american great plains village sites. *Archaeological Prospection* 2003;10(2):131–142. URL: <http://dx.doi.org/10.1002/arp.207>. doi:10.1002/arp.207.
- Pérez-Gracia, V., Caselles, J., Clapes, J., Osorio, R., Martínez, G., Canas, J.. Integrated near-surface geophysical survey of the Cathedral of Mallorca. *Journal of Archaeological Science* 2009;36(7):1289–1299. URL: <http://www.sciencedirect.com/science/article/pii/S0305440309000867>.
- Papadopoulos, N.G., Sarris, A., Salvi, M.C., Dederix, S., Soupios, P., Dikmen, U.. Rediscovering the small theatre and amphitheatre of ancient ierapytna (SE Crete) by integrated geophysical methods. *Journal of Archaeological Science* 2012;39(7):1960–1973. URL: <http://www.sciencedirect.com/science/article/pii/S0305440312000647>.
- Ranieri, G., Godio, A., Loddo, F., Stocco, S., Casas, A., Capizzi, P., et al. Geophysical prospection of the Roman city of Pollentia, Alcúdia (Mallorca, Balearic Islands, Spain). *Journal of Applied Geophysics* 2016;134:125 – 135. URL: <http://www.sciencedirect.com/science/article/pii/S0926985116302397>. doi:<http://dx.doi.org/10.1016/j.jappgeo.2016.08.009>.
- Porée, A.A.. *Histoire de l'abbaye du Bec*. 1901.
- Gazeau, V.. Normania monastica - Prosopographie des abbés bénédictins (Xe-XIIe siècle). Caen; 2007.
- Bignot, G., Bigot, A., Biochet, G., Bucaille, E., Cayeux, E., Chaput, E., et al. Carte gologique 1/50000 de Brionne (76). 122; 1984. URL: <http://infoterre.brgm.fr>.
- Palacky, G.. Resistivity characteristics of geologic targets. *SEG* 1988;1:53–129.
- Germain, M., Peigné-Delacourt, A.. Reproduction du Monasticon Gallicanum : Collection (par Dom Michel Germain) de 168 planches de vues topographiques représentant les monastères de l'ordre de Saint-Benoît - Congrégation de Saint-Maur. Frbnf30500536 ed.; 1870. URL: <http://catalogue.bnf.fr/ark:/12148/cb30500536m.public>.
- Daniels, D.J.. Ground Penetrating Radar (2nd Edition). Institution of Engineering and Technology, HERTS.MPG Books, Bodmin, UK, 2nd edition; 2004. ISBN 978-0-86341-360-5. URL: [http://www.knovel.com/web/portal/browse/display?\\_EXT\\_KNOVEL\\_DISPLAY\\_bookid=1244](http://www.knovel.com/web/portal/browse/display?_EXT_KNOVEL_DISPLAY_bookid=1244).
- Yaliner, C., Bano, M., Kadioglu, M., Karabacak, V., Meghraoui, M., Altunel, E.. New temple discovery at the archaeological site of nysa (western turkey) using gpr method. *Journal of Archaeological Science* 2009;36(8):1680 – 1689. URL: <http://www.sciencedirect.com/science/article/pii/S0305440308003245>. doi:<https://doi.org/10.1016/j.jas.2008.12.016>.
- Castaldo, R., Crocco, L., Fedi, M., Garofalo, B., Persico, R., Rossi, A., et al. Gpr microwave tomography for diagnostic analysis of archaeological sites: the case of a highway construction in pontecagnano (southern italy). *Archaeological Prospection* 2009;16(3):203–217. URL: <http://dx.doi.org/10.1002/arp.362>. doi:10.1002/arp.362.
- Booth, A.D., Linford, N.T., Clark, R.A., Murray, T.. Three-dimensional, multi-offset ground-penetrating radar imaging of archaeological targets. *Archaeological Prospection* 2008;15(2):93–112. URL: <http://dx.doi.org/10.1002/arp.327>. doi:10.1002/arp.327.
- Trinks, I., Johansson, B., Gustafsson, J., Emilsson, J., Friberg, J., Gustafsson, C., et al. Efficient, large-scale archaeological prospection using a true three-dimensional ground-penetrating radar array system. *Archaeological Prospection* 2010;17(3):175–186. URL: <http://dx.doi.org/10.1002/arp.381>. doi:10.1002/arp.381.
- Ranieri, G., Trogu, A., Loddo, F., Piroddi, L., Zucca, R.. Geophysics-an essential tool for modern archaeology. a case from monte prama

- (sardinia, italy). 2015.
- 435 Chianese, D., D'Emilio, M., Di Salvia, S., Lapenna, V., Ragosta, M., Rizzo, E.. Magnetic mapping, ground penetrating radar surveys and magnetic susceptibility measurements for the study of the archaeological site of serra di vaglio (southern italy). *Journal of Archaeological Science* 2004;31(5):633–643. URL: <http://www.sciencedirect.com/science/article/pii/S0305440303001742>.
- Barton, K., Fenwick, J.. Geophysical investigations at the ancient royal site of rathcroghan, county roscommon, ireland. *Archaeological Prospection* 2005;12(1):3–18. URL: <https://onlinelibrary.wiley.com/doi/abs/10.1002/arp.242>. doi:10.1002/arp.242.
- 440 arXiv:<https://onlinelibrary.wiley.com/doi/pdf/10.1002/arp.242>.
- Dalan, R.A.. A review of the role of magnetic susceptibility in archaeogeophysical studies in the usa: recent developments and prospects. *Archaeological Prospection* 2008;15(1):1–31. URL: <http://dx.doi.org/10.1002/arp.323>. doi:10.1002/arp.323.
- Dahlin, T., Zhou, B.. A numerical comparison of 2d resistivity imaging with 10 electrode arrays. *Geophysical Prospecting* 2004;52(5):379–398. doi:10.1111/j.1365-2478.2004.00423.x.
- 445 Loke, M.. Electrical imaging surveys for environmental and engineering studies 2001;.
- Loke, M., Barker, R.. Rapid least-squares inversion of apparent resistivity pseudosections by a quasi-newton method1. *Geophysical Prospecting* 1996;44(1):131–152. URL: <http://dx.doi.org/10.1111/j.1365-2478.1996.tb00142.x>.
- Dahlin, T.. 2d resistivity surveying for environmental and engineering applications. *First break* 1996;14(7):275–283.
- Vega, M.D.L., Osella, A., Lascano, E.. Joint inversion of wenner and dipole-dipole data to study a gasoline-contaminated soil. *Journal of Applied Geophysics* 2003;54(1):97 – 109. URL: <http://www.sciencedirect.com/science/article/pii/S0926985103001010>. doi:<https://doi.org/10.1016/j.jappgeo.2003.08.020>.
- Athanasiou, E., Tsurlos, P., Papazachos, C., Tsokas, G.. Combined weighted inversion of electrical resistivity data arising from different array types. *Journal of Applied Geophysics* 2007;62(2):124 – 140. URL: <http://www.sciencedirect.com/science/article/pii/S0926985106001339>. doi:<https://doi.org/10.1016/j.jappgeo.2006.09.003>.
- 450 Deshayes, G.. Le Bec- Hellouin (Normandie, Eure), "Abbaye". Département de l'Eure; Mission Archéologique Départementale de l'Eure, Le Viel Evreux.; 2017. 238 p.
- Camerlynck, C., Dabas, M., Panissod, C.. Comparison between gpr and four electromagnetic methods for stone features characterization: An example. *Archaeological Prospection* 1994;1(1):5–17. doi:10.1002/1099-0763(199411)1:1.